JACS
JOURNAL OF THE AMERICAN CHEMICAL SOCIETY
Article
pubs.acs.org/JACS

Capturing the Long-Sought Small-Bandgap Endohedral Fullerene $Sc_3N@C_{82}$ with Low Kinetic Stability

Tao Wei,[†] Song Wang,[†] Fupin Liu,[†] Yuanzhi Tan,[‡] Xianjun Zhu,[†] Suyuan Xie,[‡] and Shangfeng Yang*[,†]

[†]Hefei National Laboratory for Physical Sciences at Microscale, CAS Key Laboratory of Materials for Energy Conversion, Department of Materials Science and Engineering, Synergetic Innovation Center of Quantum Information & Quantum Physics, University of Science and Technology of China, Hefei 230026, China

[‡]State Key Laboratory of Physical Chemistry of Solid Surfaces and Department of Chemistry, College of Chemistry and Chemical Engineering, Xiamen University, Xiamen 361005, China

Supporting Information

ABSTRACT: The long-sought small-bandgap endohedral fullerene $Sc_3N@C_{82}$ with low kinetic stability has been successfully synthesized and isolated for the first time, for which the molecular structure has been unambiguously determined as $Sc_3N@C_{82}$-C_{2v}(39718) by single crystal X-ray diffraction. The C_{82}-C_{2v}(39718) (or labeled as C_{82}-C_{2v}(9) according to the conventional numbering of the isolated pentagon rule (IPR) isomers based on the Fowler−Monolopoulos spiral algorithm) isomeric cage of $Sc_3N@C_{82}$ agrees well with its most stable isomer previously predicted by DFT computations and is dramatically different to those of the reported counterparts $M_3N@C_{82}$−C_s(39663) (M = Gd, Y) based on a non-IPR C_{82} isomer, revealing the strong dependence of the cage isomeric structure on the size of the encaged metal for C_{82}-based metal nitride clusterfullerenes (NCFs).

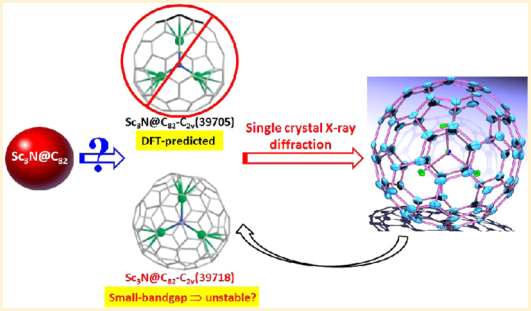

INTRODUCTION

Endohedral fullerenes are a special class of fullerenes with versatile species such as atoms, ions, or clusters encaged in their hollow, and exhibit a variety of fascinating electronic and physical/chemical properties which promise their potential applications in electronics and biomedicines, etc.[1] Among all endohedral fullerenes known so far, C_{82}-based endohedral fullerenes are quite unique because not only $La@C_{82}$ represent the first stable and separable endohedal fullerene[2] but also C_{82} cage becomes the most intensively studied and popular cage of endohedral fullerenes.[3−5] In addition to the conventional mono- and dimetallofullerenes, C_{82} cages have been also found to encapsulate different metal clusters such as nitride, carbide, sulfide, and cyanide to form clusterfullerenes.[4−7] In particular, $Sc_3N@C_{82}$ as an intriguing member of the scandium (Sc)-metal nitride clusterfullerenes (NCF) family has been detected by mass spectroscopy by different groups focusing on study of other Sc-based endohedral fullerenes,[8,9] but has never been isolated. This is dramatically different to $Sc_3N@C_{80}$ which is the first NCF discovered in 1999 (ref 10) and has been extensively studied due to its highest yield among all endohedral fullerenes isolated up to now.[1,7] The difficulty on the isolation of $Sc_3N@C_{82}$ is interpreted by its low kinetic stability arising from its small bandgap, which was computed to be 0.83 eV for the most stable isomer C_{82}-C_{2v}(39718) (or labeled as C_{82}-C_{2v}(9) according to the conventional numbering of the isolated pentagon rule (IPR) isomers based on the Fowler−Monolopoulos spiral algorithm[11]) predicted by DFT computations.[12] Contrarily, for C_{82}-NCFs based on other rare earth metals such as yttrium (Y),[13] the computed bandgap based on the experimentally determined isomer C_{82}-C_s(39663) was 1.51 eV.[12] Accordingly, it has been claimed in several theoretical studies that the low kinetic stability of $Sc_3N@C_{82}$ precluded its isolation.[9,12,14] Thus, it appears quite challenging to isolate the long-sought small-bandgap $Sc_3N@C_{82}$.

Herein, we report the synthesis of $Sc_3N@C_{82}$ by a modified Krätschmer−Huffman DC arc discharge method and its first successful isolation by three-step HPLC, accomplishing its unambiguous structural elucidation by single crystal X-ray diffraction. We further characterized the peculiar electronic property of $Sc_3N@C_{82}$ by UV−vis−NIR spectroscopy and electrochemistry.

RESULT AND DISCUSSION

Synthesis and Isolation of $Sc_3N@C_{82}$. $Sc_3N@C_{82}$ was synthesized by a modified Krätschmer−Huffman DC-arc discharging method using a mixture of Sc_2O_3 and graphite (molar ratio of Sc/C = 1:15) as the raw material with the addition of 400 mbar He and 10 mbar N_2 gas.[15] Several known $Sc_3N@C_{2n}$ ($2n$ = 68, 70, 78, 80) NCFs were also produced simultaneously and provide bases for comparison.[16−19] Isolation of $Sc_3N@C_{82}$ was performed by three-step high performance liquid chromatography (HPLC) (see Supporting Information

Received: January 9, 2015
Published: February 7, 2015

DOI: 10.1021/jacs.5b00199
J. Am. Chem. Soc. 2015, 137, 3119−3123

S1 for details). The high purity of the isolated $Sc_3N@C_{82}$ is confirmed by laser desorption time-of-flight (LD-TOF) mass spectroscopic (MS) analysis, which further confirms its proposed chemical formula based on the good agreement of the measured isotope distribution with the calculated one (see Supporting Information, Figure S2). The yield of $Sc_3N@C_{82}$ is estimated to be only 0.62% of that of $Sc_3N@C_{80}$ (I, I_h) but 3.4 times higher than that of $Sc_3N@C_{70}$-C_{2v}(7854) which is the latest member of Sc-NCF family isolated by us in 2007 (see Supporting Information S2).[10,17] Note that, in our initial attempt to synthesize $Sc_3N@C_{82}$ in a fullerene generator with a large-volume vacuum chamber (~0.048 m^3), $Sc_3N@C_{82}$ was detected in the extract mixture by mass spectroscopy but disappeared in the second-step HPLC isolation, suggesting its low stability as concluded previously in the literature.[8,9,12] After changing to a smaller-volume (~0.017 m^3) fullerene generator, we succeeded in collecting a macroscopic amount of pure $Sc_3N@C_{82}$ after the three-step HPLC isolation, suggesting a dramatically improved yield of $Sc_3N@C_{82}$ in our smaller-volume fullerene generator, presumably due to a more suitable temperature gradient for its formation.

Molecular Structure of $Sc_3N@C_{82}$ Determined by Single Crystal X-ray Diffraction. The molecular structure of $Sc_3N@C_{82}$ was determined unambiguously as $Sc_3N@C_{82}$-C_{2v}(39718) by an X-ray crystallographic study. A high-quality cubic cocrystal of $Sc_3N@C_{82}$ with Ni^{II}(OEP) (OEP = octaethylporphyrin) with a chemical form of $Sc_3N@C_{82}$·Ni^{II}(OEP)·$2C_6H_6$ was obtained by diffusion of a carbon disulfide solution of $Sc_3N@C_{82}$ into a benzene solution of Ni^{II}(OEP) and used for X-ray crystallographic study.[3,6,10,20−23] Figure 1 shows the relative orientations of the $Sc_3N@C_{82}$-C_{2v}(39718) and the Ni^{II}(OEP) molecules in $Sc_3N@C_{82}$-C_{2v}(39718)·Ni^{II}(OEP)·$2C_6H_6$. Only one orientation of the fullerene cage together with the major site of the Sc_3N cluster was shown in the drawing for clarity. Like most of the previously reported cocrystals of versatile NCFs with Ni^{II}(OEP),[21−23] the $Sc_3N@C_{82}$-C_{2v}(39718)·Ni^{II}(OEP)·$2C_6H_6$ cocrystal was monoclinic with a space group of $C2/m$. Thus, its asymmetric unit cell contains a half of the Ni^{II}(OEP) molecule and two halves of the C_{2v}(39718)-C_{82} cage. An intact C_{82} cage can be finally formed by combining one of the halves of the fullerene cage with the mirror image of the other. Accordingly, two orientations of the carbon cage with the same occupancies of 0.5 can be inferred. The fully ordered Ni^{II}(OEP) molecule resides on the crystallographic mirror plane that bisects N2, Ni, and N4, so an entire Ni^{II}(OEP) molecule can be formed by combining the existing half molecule with its mirror image. The shortest distance between the carbon cage involving C76 and the nickel ion in Ni^{II}(OEP) is 2.972(2) Å, which is comparable to those reported for other cocrystals of NCFs and Ni^{II}(OEP).[23]

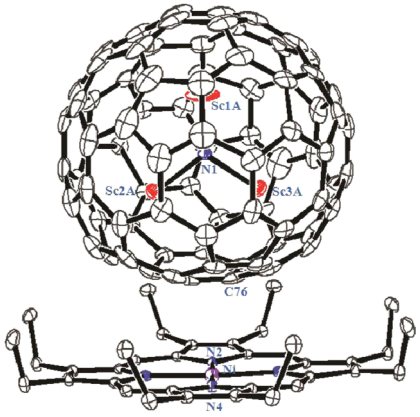

Figure 1. Drawing showing the orientation of endohedral fullerene with respect to nickel porphyrin in $Sc_3N@C_{82}$-C_{2v}(39718)·Ni^{II}(OEP)·$2C_6H_6$ with 30% thermal ellipsoids. Only one orientation of the fullerene cage (0.50 occupancy) and the major site of Sc_3N are shown. C, N, Sc, and Ni atoms are shown in gray, blue, red and purple, respectively. The solvent molecule (benzene), another orientation of the fullerene cage, the minor site of Sc_3N, and hydrogen atoms of the porphyrin are all omitted for clarity.

Inside the C_{82}-C_{2v}(39718) cage, which follows IPR and can be labeled as C_{82}-C_{2v}(9) according to the Fowler−Monolopoulos spiral algorithm,[11] the encaged Sc_3N cluster shows disorder with two sites, while the central nitrogen atom is fully ordered which is situated on the mirror plane of the entire molecule. This case is similar to that of $Sc_3N@C_{80}$ (I, I_h) but obviously different from that of $Sc_3N@C_{68}$-D_3(6140) with as many as 13 Sc sites.[10,16] For the major site of the Sc_3N cluster, Sc1A with an occupancy of 0.712(4) is located on the mirror plane of the entire molecule, while Sc2A and its mirror image labeled as Sc3A with an equal occupancy of 0.444(3) are symmetrically situated in two sides of the cage. The minor Sc_3N site comprises Sc1B, Sc2B, and Sc3B with an occupancy of 0.218(2), 0.556(4), and 0.556(4), respectively (see Supporting Information, Figure S3a for its relative orientation to the major Sc_3N site). Interestingly, as clearly shown in Figure 2 illustrating the positions of three Sc atoms within the major Sc_3N site with respect to the neighboring portions of the C_{82}-C_{2v}(39718) cage, the three Sc atoms (Sc1A−Sc3A) are all located at the conjunctions of pentagons and hexagons. This is quite different to the case of the counterpart $Gd_3N@C_{82}$-C_s(39663) with a non-IPR egg-shaped cage containing one fused pentagon pair, within which the Gd1 atom (major site) is located under the pentalene fold while Gd2 and Gd3 were observed at the conjunction of pentagon/hexagon and under a pentagon, respectively.[20] The different locations of the encaged metal atoms within the C_{82} cage suggest the difference in the cluster-cage interactions between $Sc_3N@C_{82}$ and $Gd_3N@C_{82}$ as predicted in a previous DFT computational study.[12]

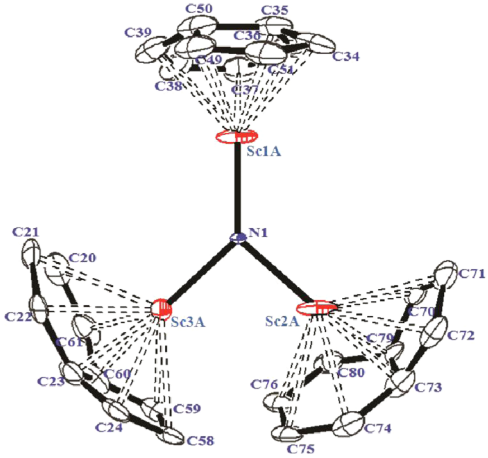

Figure 2. Position of the major Sc_3N site with respect to the nearest carbon atoms of the C_{2v}(39718)-C_{82} cage. C, N, and Sc atoms are shown in gray, blue, and red, respectively.

DOI: 10.1021/jacs.5b00199
J. Am. Chem. Soc. 2015, 137, 3119−3123

For the major site of Sc3N cluster, the Sc1A−N1−Sc2A/Sc3A and Sc2A−N1−Sc3A angles are 132.13(9)° and 95.23(7)°, respectively. Thus, the sum of these three angles about the central nitrogen atom is 359.49°, indicating that the encaged Sc_3N cluster is planar. This feature is similar to that for the Gd_3N cluster within $Gd_3N@C_{82}$-C_s(39663).[20] The Sc1A−N1 and Sc2A/Sc3A−N1 bond distances are 2.007(4) Å and 2.078(3) Å, respectively, and Sc1A−N distance is obviously shorter than those within $Gd_3N@C_{82}$-C_s(39663) (2.077(5), 2.094(5), 2.152(5) for the major Gd sites).[20] This result can be explained by the much smaller ionic radius of Sc^{3+} (0.75 Å) than that of Gd^{3+} (0.94 Å).[24] On the other hand, the averaged Sc−N distance based on Sc1A−N1 and Sc2A/Sc3A−N1 bond distances within $Sc_3N@C_{82}$-C_{2v}(39718) is 2.054 Å, which is slightly smaller than that computed by DFT (2.062 Å).[12]

C_{82}-based NCFs have been rarely reported and so far only four $M_3N@C_{82}$ (M = Y,[13] Gd,[20] Dy,[25] Tm[26]) NCFs have been isolated, among which only $Gd_3N@C_{82}$-C_s(39663) and $Y_3N@C_{82}$-C_s(39663) have been structurally characterized and share the same non-IPR C_{82}-C_s(39663) isomeric cage.[13,20] This is no wonder considering the relatively close ionic radii of Gd^{3+} (0.94 Å) and Y^{3+} (0.90 Å).[24] However, upon decreasing the size of the encaged metal from Y to Sc, $Sc_3N@C_{82}$ has a dramatic different isomeric cage structure of C_{82}-C_{2v}(39718), revealing the strong dependence of the cage isomeric structure on the size of the encaged metal for C_{82}-based NCFs. As already concluded in a previous comparative study of a series of C_{80}-based NCFs $M_3N@C_{80}$ (I_h, M = Sc, Y, Gd, Tb, Dy, Ho, Er, Tm), the much smaller ionic radius of Sc^{3+} (0.75 Å) than those of other rare earth metals resulted in weaker charge transfer from the Sc_3N cluster to the C_{80} cage and consequently weaker cluster-cage interactions within $Sc_3N@C_{80}$ compared to those in other $M_3N@C_{80}$ NCFs. Despite such weaker cluster-cage interactions within $Sc_3N@C_{80}$, its cage isomeric structure (C_{80}-I_h) remains same to those of other $M_3N@C_{80}$ NCFs.[21] For the case of the C_{82} cage, the increase of the cage size leads to the weakening of the cluster-cage interactions within $M_3N@C_{82}$ NCFs and consequently induces more dramatic deviation of $Sc_3N@C_{82}$ from other $M_3N@C_{82}$ NCFs in terms of the stability order of the isomers as revealed in a previous DFT computational study of C_{82}-based NCFs by Popov and Dunsch.[12] Interestingly, DFT computations on $Sc_3N@C_{82}$ predicted that C_{82}-C_{2v}(39718) was the most stable isomer but had a low kinetic stability as inferred from its small highest occupied molecular orbital−lowest unoccupied molecular orbital (HOMO−LUMO) gap of 0.83 eV, thus the candidate for $Sc_3N@C_{82}$ was suggested to be the second most stable isomer, non-IPR C_{82}-C_{2v}(39705), instead of C_{82}-C_{2v}(39718).[12] Therefore, the successful isolation and unambiguous structural determination of $Sc_3N@C_{82}$-C_{2v}(39718) in our present work unravels the long-lasting puzzle about its molecular structure and proves the possibility of isolating such a small-bandgap endohedral fullerene with low kinetic stability.

Furthermore, the dramatic difference on the isomeric cage structures of $Sc_3N@C_{82}$-C_{2v}(39718) and $M_3N@C_{82}$-C_s(39663) (M = Gd, Y) is consistent with that predicted by a previous DFT computational study.[12] Specifically, $Y_3N@C_{82}$ isomers exhibited significantly different stability order to that for $Sc_3N@C_{82}$, with C_{82}-C_{2v}(39705) being the most stable isomer. However, it is the second most stable isomer, C_{82}-C_s(39663), that was later confirmed to be the cage of the experimentally isolated $Y_3N@C_{82}$.[12,13] Such a discrepancy between the experimentally determined isomeric structure with the computationally predicted most stable one however does not exist for $Sc_3N@C_{82}$, confirming further the role of the encaged metal on the cage isomeric structure of C_{82}-based NCFs. Given that cages larger than C_{82} have been isolated for NCFs based on many lanthanide metals such as La, Gd, Dy, Tm etc.,[25−28] it remains an open question whether Sc-based NCFs with cages larger than C_{82} follows the similar dependence or not. We expect that our present work will stimulate such interesting studies.

Electronic Absorption Spectroscopic Study of $Sc_3N@C_{82}$. The UV−vis−NIR absorption spectrum of the isolated $Sc_3N@C_{82}$-C_{2v}(39718) dissolved in toluene is presented in Figure 3. The electronic absorption spectrum of $Sc_3N@C_{82}$

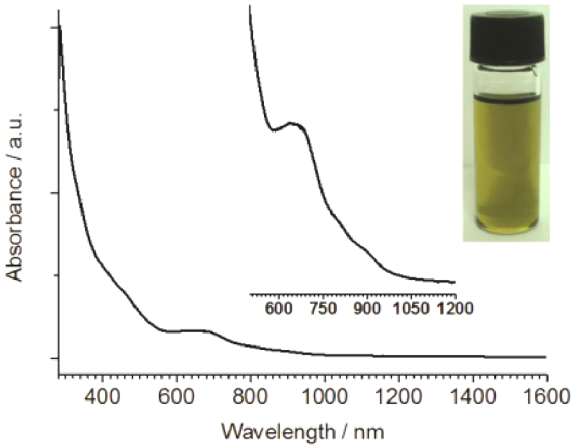

Figure 3. UV−vis−NIR spectrum of $Sc_3N@C_{82}$-C_{2v}(39718) dissolved in toluene. Insets: enlarged spectral region (500−1200 nm) and the photograph of sample in toluene.

exhibits two broad shoulder peaks at about 341 and 465 nm along with one clearly discernible broad peak with the absorption maximum at about 642 nm in the UV and visible regions. Besides, an additional weak broad shoulder absorption peak appears at about 908 nm in the NIR region. Because of such a unique electronic absorption feature, $Sc_3N@C_{82}$ solution in toluene is green (see inset of Figure 3). The electronic absorption feature of $Sc_3N@C_{82}$-C_{2v}(39718) is apparently different from that of $Gd_3N@C_{82}$-C_s(39663) which exhibits four broad shoulder absorption peaks (343, 386, 501, 643 nm) in the visible region only.[20] The obvious difference in the electronic absorption properties between $Sc_3N@C_{82}$-C_{2v}(39718) and $Gd_3N@C_{82}$-C_s(39663) can be easily understood by their discrepancy on the cage isomeric structure since the electronic absorptions of fullerenes are predominantly due to $\pi-\pi^*$ carbon cage transitions and primarily depend on the isomeric structure and charge state of the carbon cage.[1,7] More strikingly, the optical bandgap of $Sc_3N@C_{82}$-C_{2v}(39718) estimated from its absorption spectral onset of ca. 1696 nm (see Supporting Information, Figure S4) is 0.73 eV, which is again significantly smaller than that of $Gd_3N@C_{82}$-C_s(39663).[20] Besides, the optical band gap of $Sc_3N@C_{82}$-C_{2v}(39718) is also much smaller than those of the other reported members of the Sc-based NCF family including $Sc_3N@C_{2n}$ ($2n$ = 68, 70, 78, 80) which are all not lower than 1.0 eV (see Supporting Information, Table S3).[16−19] Such a small optical bandgap of $Sc_3N@C_{82}$-C_{2v}(39718) confirms its low kinetic stability as predicted by DFT computation[11] and explains the difficulty in its isolation as the long-sought member of the Sc-based NCF family. To evaluate the thermal stability of $Sc_3N@C_{82}$, we heated a

DOI: 10.1021/jacs.5b00199
J. Am. Chem. Soc. 2015, 137, 3119−3123

$Sc_3N@C_{80}$ solution in reflux toluene under ambient condition and detected the peak intensity by HPLC, and found that, while the peak intensity of $Sc_3N@C_{82}$ remained unchanged under heating at 150 °C for 90 min, it decreased obviously under heating at 180 °C for 90 min, suggesting its decomposition at this temperature. However, a similar heating treatment of $Sc_3N@C_{80}$ solution in reflux toluene revealed that its HPLC peak intensity remained unchanged under heating at 180 °C for 90 min, confirming its higher thermal stability than $Sc_3N@C_{82}$ (see Supporting Information, Figure S5).

Electrochemical Study of $Sc_3N@C_{82}$. Figure 4 presents a typical cyclic voltammogram of $Sc_3N@C_{82}$-C_{2v}(39718) measured in *o*-dichlorobenzene (*o*-DCB) with tetrabutylammonium hexafluorophosphate ($TBAPF_6$) as supporting electrolyte. The characteristic redox potentials are summarized in Supporting Information, Table S4, which also includes those of $Gd_3N@C_{82}$-C_s(39663)[29] for comparison. In the anodic region, $Sc_3N@C_{82}$-C_{2v}(39718) exhibits two reversible oxidation steps with half-wave potentials ($E_{1/2}$) at 0, 0.37 V, respectively. Such oxidation behavior is obviously different from that of $Gd_3N@C_{82}$-C_s(39663) with only one reversible oxidation step ($E_{1/2,ox}$ = 0.37 V).[29] The more negative first oxidation potential of $Sc_3N@C_{82}$-C_{2v}(39718) compared to that of $Gd_3N@C_{82}$-C_s(39663) suggests its stronger electron-donating ability. On the other hand, in the cathode region, $Sc_3N@C_{82}$-C_{2v}(39718) shows a complex reduction behavior with up to four reduction steps. While the first reduction step of $Sc_3N@C_{82}$-C_{2v}(39718) was distinctly irreversible with a peak potential (E_p) at −1.35 V, which is positively shifted compared to that of $Gd_3N@C_{82}$-C_s(39663) (−1.52 V),[29] the second-fourth reduction steps become more reversible with half-wave potentials ($E_{1/2,\,red}$) at −1.52, −1.78, and −2.18 V, respectively. Again, the reduction behavior of $Sc_3N@C_{82}$-C_{2v}(39718) is obviously different from that of $Gd_3N@C_{82}$-C_s(39663) which shows only two reduction steps.[28] The electrochemical gap ($E_{gap,ec}$), derived from the distinct discrepancy of the redox behavior specifically of the first oxidation and reduction potentials between $Sc_3N@C_{82}$-C_{2v}(39718) and $Gd_3N@C_{82}$-C_s(39663), shows quite a large difference (0.54 V, see Supporting Information, Table S4). This is consistent with the difference in their optical bandgap of the structures as discussed above and can be attributed to their discrepancy in the cage isomeric structure.

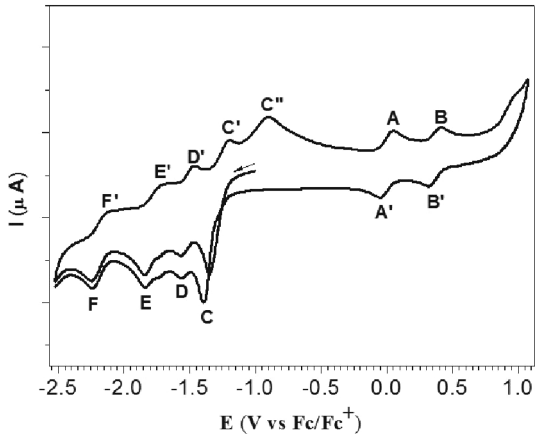

Figure 4. Cyclic voltammogram of $Sc_3N@C_{82}$-C_{2v}(39718) in *o*-DCB solution with ferrocene (Fc) as the internal standard and $TBAPF_6$ as the supporting electrolyte. Scan rate, 100 mV/s. The letters A and B mark the oxidation peaks and their corresponding rereduction peaks are marked by A′, B′. The oxidation and rereduction peaks of ferrocene (Fc) coincidentally overlap with peaks A and A′, respectively. Letters C−F label the first to fourth reduction peaks and their corresponding reoxidation peaks are labeled by C′−F′ and C″.

CONCLUSION

In summary, we have successfully synthesized and isolated the long-sought $Sc_3N@C_{82}$ for the first time, which has been claimed in several theoretical studies to have low kinetic stability precluding its isolation. The molecular structure of $Sc_3N@C_{82}$ has been unambiguously determined as $Sc_3N@C_{82}$-C_{2v}(39718) by single crystal X-ray diffraction, ruling out the isomeric structure of non-IPR C_{82}-C_{2v}(39705) previously predicted by DFT computations. The determined C_{82}-C_{2v}(39718) isomeric cage of $Sc_3N@C_{82}$ follows IPR and is consistent with its DFT-predicted most stable isomer, but is dramatically different from those of the reported analogous NCFs $M_3N@C_{82}$-C_s(39663) (M = Gd, Y) based on a non-IPR C_{82} isomer, revealing the strong dependence of cage isomeric structure on the size of the encaged metal for C_{82}-based NCFs. The optical bandgap of $Sc_3N@C_{82}$-C_{2v}(39718) estimated from a UV−vis−NIR spectroscopic study is 0.73 eV, much smaller than those of $Gd_3N@C_{82}$-C_s(39663) and $Sc_3N@C_{2n}$ (2*n* = 68, 70, 78, 80), confirming its relatively low kinetic stability resulting in the difficulty in its isolation. A cyclic voltammetric study of $Sc_3N@C_{82}$-C_{2v}(39718) reveals a complex redox behavior which is dramatically different from that of $Gd_3N@C_{82}$-C_s(39663). Our success in the first isolation of $Sc_3N@C_{82}$ unravels the long-lasting puzzle about its molecular structure, and will stimulate further study on such seemingly unstable endohedral fullerenes toward deeper understanding of the dependence of the stability of endohedral fullerene on its cage isomeric structure.

EXPERIMENTAL METHODS

Synthesis and Isolation of $Sc_3N@C_{82}$-C_{2v}(39718). The synthesis of $Sc_3N@C_{82}$-C_{2v}(39718) by a modified Krätschmer−Huffman DC-arc discharging method involving N_2 gas follows the similar procedures of synthesizing other Sc-based NCFs reported previously.[15] The produced soot was collected and Soxhlet-extracted by CS_2 for 24 h. The resulting brown-yellow solution was distilled to remove CS_2 and then immediately redissolved in toluene and subsequently passed through a 0.2 μm Telflon filter (Sartorius AG, Germany) for HPLC separation. Isolation of $Sc_3N@C_{82}$ was performed by three-step HPLC as described in details in Supporting Information S1. The purity of the isolated $Sc_3N@C_{82}$ was further checked by LD-TOF MS (Biflex III, Bruker Daltonics Inc., Germany).

Spectroscopic and Electrochemical Study of $Sc_3N@C_{82}$-C_{2v}(39718). UV−vis−NIR spectra were recorded on a UV−vis−NIR 3600 spectrometer (Shimadzu, Japan) using a quartz cell of 1 mm layer thickness and 1 nm resolution with the samples dissolved in toluene. An electrochemical study of $Sc_3N@C_{82}$-C_{2v}(39718) was performed in *o*-dichlorobenzene (*o*-DCB, anhydrous, 99%, Aldrich). The supporting electrolyte was tetrabutylammonium hexafluorophosphate (TBAPF6, puriss. electrochemical grade, Fluka) which was dried under reduced pressure at 340 K for 24 h and stored in glovebox prior to use. Cyclic voltammogram experiments were performed with a CHI 660 potentiostat (CHI Instrument, U.S.A.) at room temperature in a glovebox. A standard three-electrode arrangement of a platinum (Pt) wire as working electrode, a platinum coil as counter electrode, and a silver wire as a pseudoreference electrode was used. In a comparison experiment, ferrocene (Fc) was added as the internal standard and all potentials are referred to the Fc/Fc^+ couple.

X-ray Crystallographic Study of $Sc_3N@C_{82}$-C_{2v}(39718). Crystal growth of $Sc_3N@C_{82}$-C_{2v}(39718)·Ni^{II}(OEP)·$2C_6H_6$ was accomplished by layering a solution of 1 mg Ni^{II}(OEP) in 1 mL of benzene over a solution of ca. 2 mg of $Sc_3N@C_{82}$-C_{2v}(39718) in 2 mL of carbon

DOI: 10.1021/jacs.5b00199
J. Am. Chem. Soc. 2015, 137, 3119−3123

disulfide. X-ray diffraction data collection for the crystal of $Sc_3N@C_{82}$·$Ni^{II}(OEP)$·$2C_6H_6$ ($0.1 \times 0.08 \times 0.06$ mm^3) was carried out at 100 K on an Agilent Supernova diffractometer (Agilent Technologies, U.S.A.) with a Cu radiation (λ = 1.54178 Å). $Sc_3N@C_{82}$·$Ni^{II}(OEP)$·$2C_6H_6$ crystallizes in the monoclinic space group $C2/m$, a = 25.2209(5) Å, b = 15.1985(3) Å, c = 19.9181(4) Å, β = 94.772(2)°, V = 7608.5(3) Å^3, Z = 4. A numerical absorption correction utilizing equivalents was employed. The structure was solved by direct methods and refined using all data (based on F^2) by SHELX 97.[30] Hydrogen atoms were located in a difference map, added geometrically, and refined with a riding model. Refinement of 7517 reflections, 1034 parameters, and 1075 restraints yielded wR2 = 0.2034 for all data and a conventional R1 of 0.0721 based on 6807 reflections with $I > 2\sigma(I)$. These data can be obtained free of charge from the Cambridge Crystallographic Data Centre with CCDC No. 1034177.

■ ASSOCIATED CONTENT

Supporting Information

Isolation of $Sc_3N@C_{82}$-C_{2v}(39718); estimation of the relative yield of $Sc_3N@C_{82}$; X-ray crystallographic data of $Sc_3N@C_{82}$-C_{2v}(39718); UV−vis−NIR spectrum of $Sc_3N@C_{82}$ in CS_2 solution; thermal stability of $Sc_3N@C_{82}$ vs $Sc_3N@C_{80}$-I_h; cyclic voltammograms of $Sc_3N@C_{82}$-C_{2v}(39718) in different scanning regions; and X-ray crystallographic files in CIF formats etc. This material is available free of charge via the Internet at http://pubs.acs.org.

■ AUTHOR INFORMATION

Corresponding Author

sfyang@ustc.edu.cn

Notes

The authors declare no competing financial interest.

■ ACKNOWLEDGMENTS

This work was partially supported by the National Natural Science Foundation of China (Grant Nos. 21132007, 2137116), National Basic Research Program of China (Grant No. 2011CB921400) (to S.F.Y.), the 973 project (2014CB845601) and the National Natural Science Foundation of China (Grant No. U1205111) (to S.Y.X.).

■ REFERENCES

(1) For recent reviews, see (a) Yang, S. F., Wang, C. R. *Endohedral Fullerenes: From Fundamentals to Applications*; World Scientific Publishing Co. Pte. Ltd.: Singapore, 2014. (b) Popov, A. A.; Yang, S. F.; Dunsch, L. *Chem. Rev.* **2013**, *113*, 5989. (c) Wang, T. S.; Wang, C. R. *Acc. Chem. Res.* **2014**, *47*, 450. (d) Lu, X.; Feng, L.; Akasaka, T.; Nagase, S. *Chem. Soc. Rev.* **2012**, *41*, 7723. (e) Yang, S. F. *Curr. Org. Chem.* **2012**, *16*, 1079. (f) Rodriguez-Fortea, A.; Balch, A. L.; Poblet, J. M. *Chem. Soc. Rev.* **2011**, *40*, 3551. (g) Yang, S. F.; Liu, F. P.; Chen, C. B.; Jiao, M. Z.; Wei, T. *Chem. Commun.* **2011**, *47*, 11822. (h) Chaur, M. N.; Melin, F.; Ortiz, A. L.; Echegoyen, L. *Angew. Chem., Int. Ed.* **2009**, *48*, 7514.

(2) Chai, Y.; Guo, T.; Jin, C.; Haufler, R. E.; Chibante, L. P. F.; Fure, J.; Wang, L.; Alford, G. M.; Smalley, R. E. *J. Phys. Chem.* **1991**, *95*, 7564.

(3) (a) Xu, W.; Niu, B.; Feng, L.; Shi, Z.; Lian, Y. *Chem.—Eur. J.* **2012**, *18*, 14246. (b) Yang, H.; Jin, H.; Wang, X.; Liu, Z.; Yu, M.; Zhao, F.; Mercado, B. Q.; Olmstead, M. M.; Balch, A. L. *J. Am. Chem. Soc.* **2012**, *134*, 14127. (c) Suzuki, M.; Slanina, Z.; Mizorogi, N.; Lu, X.; Nagase, S.; Olmstead, M. M.; Balch, A. L.; Akasaka, T. *J. Am. Chem. Soc.* **2012**, *134*, 18772.

(4) (a) Lu, X.; Nakajima, K.; Iiduka, Y.; Nikawa, H.; Mizorogi, N.; Slanina, Z.; Tsuchiya, T.; Nagase, S.; Akasaka, T. *J. Am. Chem. Soc.* **2011**, *133*, 19553. (b) Zhang, J.; Fuhrer, T.; Fu, W.; Ge, J.; Bearden, D. W.; Dallas, J.; Duchamp, J. C.; Walker, K. L.; Champion, H.; Azurmendi, H. F.; Harich, K.; Dorn, H. C. *J. Am. Chem. Soc.* **2012**, *134*, 8487. (c) Wang, C.; Kai, T.; Tomiyama, T.; Yoshida, T.; Kobayashi, Y.; Nishibori, E.; Takata, M.; Sakata, M.; Shinohara, H. *Angew. Chem., Int. Ed.* **2001**, *46*, 397.

(5) Dunsch, L.; Yang, S.; Zhang, L.; Svitova, A.; Oswald, S.; Popov, A. A. *J. Am. Chem. Soc.* **2010**, *132*, 5413.

(6) (a) Yang, S. F.; Chen, C. B.; Liu, F. P.; Xie, Y. P.; Li, F. Y.; Jiao, M. Z.; Suzuki, M.; Wei, T.; Wang, S.; Chen, Z. F.; Lu, X.; Akasaka, T. *Sci. Rep.* **2013**, *3*, 1487. (b) Liu, F.; Wang, S.; Guan, J.; Wei, T.; Zeng, M.; Yang, S. *Inorg. Chem.* **2014**, *53*, 5201.

(7) (a) Zhang, J. Y.; Stevenson, S.; Dorn, H. C. *Acc. Chem. Res.* **2013**, *46*, 1548. (b) Dunsch, L.; Yang, S. F. *Small* **2007**, *3*, 1298. (c) Dunsch, L.; Yang, S. F. *Phys. Chem. Chem. Phys.* **2007**, *9*, 3067.

(8) (a) Stevenson, S.; Mackey, M. A.; Pickens, J. E.; Stuart, M. A.; Confait, B. S.; Phillips, J. P. *Inorg. Chem.* **2009**, *48*, 11685. (b) Mercado, B. Q.; Stuart, M. A.; Mackey, M. A.; Picken, J. E.s; Confait, B. S.; Stevenson, S.; Easterling, M. L.; Valencia, R.; Rodriguez-Fortea, A.; Poblet, J. M.; Olmstead, M. M.; Balch, A. L. *J. Am. Chem. Soc.* **2010**, *132*, 12098.

(9) Svitova, A. L.; Popov, A. A.; Dunsch, L. *Inorg. Chem.* **2013**, *52*, 3368.

(10) Stevenson, S.; Rice, G.; Glass, T.; Harich, K.; Cromer, F.; Jordan, M. R.; Craft, J.; Hadju, E.; Bible, R.; Olmstead, M. M.; Maitra, K.; Fisher, A. J.; Balch, A. L.; Dorn, H. C. *Nature* **1999**, *401*, 55.

(11) Fowler, P.; Manolopoulos, D. E. *An Atlas of Fullerenes*; Clarendon Press: Oxford, U.K., 1995.

(12) Popov, A. A.; Dunsch, L. *J. Am. Chem. Soc.* **2007**, *129*, 11835.

(13) Fu, W. J.; Xu, L. S.; Azurmendi, H.; Ge, J. C.; Fuhrer, T.; Zuo, T. M.; Reid, J.; Shu, C. Y.; Harich, K.; Dorn, H. C. *J. Am. Chem. Soc.* **2009**, *131*, 11762.

(14) Campanera, J. M.; Bo, C.; Poblet, J. M. *Angew. Chem., Int. Ed.* **2005**, *44*, 7230.

(15) Yang, S. F.; Chen, C. B.; Popov, A. A.; Zhang, W. F.; Liu, F. P.; Dunsch, L. *Chem. Commun.* **2009**, 6391.

(16) (a) Stevenson, S.; Fowler, P. W.; Heine, T.; Duchamp, J. C.; Ric e, G.; Glass, T.; Harich, K.; Hajdu, E.; Bible, R.; Dorn, H. C. *Nature* **2000**, *408*, 427. (b) Olmstead, M. M.; Lee, H. M.; Dunchamp, J. C.; Sevenson, S.; Marciu, D.; Dorn, H. C.; Balch, A. L. *Angew. Chem., Int. Ed.* **2003**, *115*, 928.

(17) Yang, S. F.; Popov, A. A.; Dunsch, L. *Angew. Chem., Int. Ed.* **2007**, *46*, 1256.

(18) Olmstead, M. H.; Bettencourt-Dias, A. de; Duchamp, J. C.; Stevenson, S.; Marciu, D.; Dorn, H. C.; Balch, A. L. *Angew. Chem., Int. Ed.* **2001**, *40*, 1223.

(19) Krause, M.; Dunsch, L. *ChemPhysChem* **2004**, *5*, 1445.

(20) Mercado, B. Q.; Beavers, C. M.; Olmstead, M. M.; Chaur, M. N.; Walker, K.; Holloway, B. C.; Echegoyen, L.; Balch, A. L. *J. Am. Chem. Soc.* **2008**, *130*, 7854.

(21) Yang, S. F.; Troyanov, S. I.; Popov, A. A.; Krause, M.; Dunsch, L. *J. Am. Chem. Soc.* **2006**, *128*, 16733.

(22) Zuo, T.; Olmstead, M. M.; Beavers, C. M.; Balch, A. L.; Wang, G.; Yee, G. T.; Shu, C.; Xu, L.; Elliott, B.; Echegoyen, L.; Duchamp, J. C.; Dorn, H. C. *Inorg. Chem.* **2008**, *47*, 5234.

(23) (a) Beavers, C. M.; Chaur, M. N.; Olmstead, M. M.; Echegoyen, L.; Balch, A. L. *J. Am. Chem. Soc.* **2009**, *131*, 11519. (b) Zuo, T. M.; Beavers, C. M.; Duchamp, J. C.; Campbell, A.; Dorn, H. C.; Olmstead, M. M.; Balch, A. L. *J. Am. Chem. Soc.* **2007**, *129*, 2035.

(24) Greenwood, N. N., Earnshaw, A. *Chemistry of the Elements*; Pergamon: Oxford, 1984.

(25) Yang, S. F.; Dunsch, L. *J. Phys. Chem. B* **2005**, *109*, 12320.

(26) Krause, M.; Wong, J.; Dunsch, L. *Chem.—Eur. J.* **2005**, *11*, 706.

(27) Chaur, M. N.; Melin, F.; Ashby, J.; Elliott, B.; Kumbhar, A.; Rao, A. M.; Echegoyen, L. *Chem.—Eur. J.* **2008**, *14*, 8213.

(28) Krause, M.; Dunsch, L. *Angew. Chem., Int. Ed.* **2005**, *44*, 1557.

(29) Chaur, M. N.; Athans, A. J.; Echegoyen, L. *Tetrahedron* **2008**, *64*, 11387.

(30) Sheldrick, G. *Acta Crystallogr. A* **2008**, *64*, 112.

DOI: 10.1021/jacs.5b00199
J. Am. Chem. Soc. 2015, 137, 3119−3123